

# Efficient and Accurate Analysis of a Substrate Integrated Waveguide (SIW) Rat-Race Coupler Excited by Four U-Shape Slot-Coupled Transitions

R. Dehdasht-Heydari <sup>1</sup>, K. Forooraghi <sup>2</sup>, and M. Naser-Moghadas <sup>1</sup>

<sup>1</sup> Department of Electrical Engineering, Science and Research Branch  
Islamic Azad University, Tehran, Iran  
dehdashtheydari@gmail.com, mn\_moghaddasi@yahoo.com

<sup>2</sup> Department of Electrical Engineering  
Tarbiat Modares University (TMU), Tehran, Iran  
KEYVAN\_F@modares.ac.ir

**Abstract** — In this paper, the bandwidth of one SIW rat-race (hybrid ring) coupler has been increased up to 30% by four U-shape slot-coupled transitions without disadvantages due to transmission line loss, radiation and design complexity. The SIW coupler structure has been analyzed by the mode matching method that uses the cylindrical vector expansion to minimize computational time and memory occupation. Throughout 11-15 GHz bandwidth, return loss and isolation as well as phase differences in output ports have been presented. It is observed that the numerical results are in good agreement with simulation and experimental measurement.

**Index Terms** — Boundary conditions, coaxial cables, Cylindrical Vector Waves (CVWs), Dyadic Green's Functions (DGFs), rat-race (hybrid ring) coupler, Substrate Integrated Waveguide (SIW), transition, U-shape slots.

## I. INTRODUCTION

Substrate Integrated Waveguide (SIW) structures are also known as laminated waveguide or post-wall waveguide structures. They are used as a concept for the design of microwave and millimeter-wave waveguide structures and components [1]. SIWs are based on the equivalence between well-known metallic waveguide structures (usually a Rectangular Waveguide (SIRW)) and waveguide structures on

a dielectric substrate using rows of metal posts (vias). Many passive components, such as filters, antennas, circulators, couplers, transitions, etc., are based on SIW or similar technologies, and they have been studied in [2-9].

Without any doubts, the transitions between excitation section and SIRW are mostly a critical element to get optimized S-parameters. Several transitions for the SIRW were presented [10-15] over the last few years, like transformers to rectangular waveguides, single layer transitions from microstrip lines to SIRWs, uniplanar CPW transitions, GCPW transitions. However, these structures have drawbacks such as not compatible with planar circuits, incompatible with low-loss SIRWs, radiation and design complexity and fabrication. Therefore, a new design of transition is necessary in order to simplify the structure and improve bandwidth.

Recently, several papers [16-22] have applied a Cylindrical Vector Wave expansion (CVW) to study the simplified 2-D case and the full 3-D case. These mode expansions allow an efficient full-wave analysis of SIW structures for metallic and dielectric posts. Nevertheless, there is a need in using efficient method of mode matching to analyze wideband SIW structures; for instance, SIW couplers.

The single-layer SIW rat race coupler basically has been proposed in [23], utilizing the transition from microstrip lines to SIW rat-race

arms. Accordingly, there was not mentioned anything about output phases (0 and 180 degrees) and the analysis of the coupler. This coupler has limited bandwidth (about 10% in X-band and 7% in Ka-band) and its dimensions should optimize to obtain further bandwidth.

In this paper, a simple SIW transition structure is designed for 8.5-16.5 GHz frequency (over 50% relative bandwidth) in Section II. The coaxial cables are accompanied with U-shape slots to excite the signal inside the SIW. As an application, a SIW hybrid ring coupler has been modified with this new SIW transition to increase the bandwidth over than 30% and carry out a lower loss and profile coupler. The design and optimization procedure of the coupler have been presented in Section III. In Section IV, the proposed coupler has been analyzed and the vector wave functions have been used for the coupler. By imposing boundary conditions on each post and transfer the obtained equations to the matrix, the unknown coefficients have been determined and scattering parameters of the proposed rat-race coupler to be calculated. To confirm the efficiency and accuracy of the method, the coupler calculated parameters have been compared with simulated and measured results in Section V.

## II. DESIGN OF U-SHAPE SLOT-COUPLED TRANSITION

The structure of U-shape slot-coupled transition is shown in Fig. 1. The structure is similar to conventional SIW, which is excited with coaxial cable directly with no need to use microstrip line transition. The sole difference is in rectangular U-shape slots above the substrate plate where the inner conductors of coaxial cables are connected to the top plate. In the first step, we simulated a two port SIW waveguide without coaxial probes for single-mode (i.e., TE<sub>10</sub> mode) in the operating frequency range of 8.5-16.5 GHz with CST microwave studio. In the next step, it is necessary to use the transition from two coaxial probes to the SIW waveguide. We have seen in the CST package that by using a slot coupling for probe feeding to SIW transition, the input resistance increases with the thickness of SIW substrate but decreases with slot length.

This trade off can be achieved by adjusting the length and shape of the slot. Therefore, the

transition bandwidth can be maximized by matching the input resistance as nearly as to the characteristic impedance of the probe feeding.

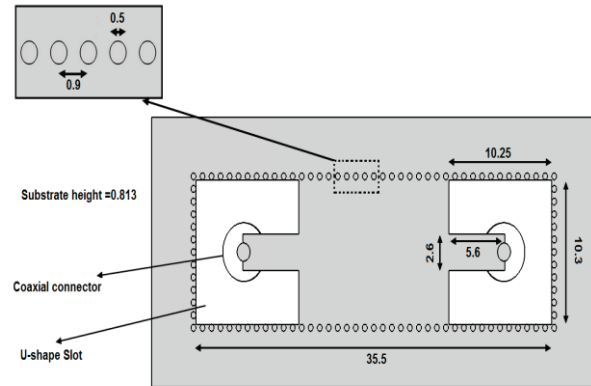


Fig. 1. The back-to-back U-shape slot-coupled transition structure (all dimensions are in millimeters).

From optimization in CST for different slot shapes along with different lengths, we realized that the best configuration to maximize the relative bandwidth of the transition can be exploited by U-shape slots rather than the other shapes (e.g., E-shape slots). Therefore, the two U-shape slots are designed to enhance the bandwidth of the SIW structure excited by coaxial cables without radiation from the slots or design complication as well as the bandwidth of the structure with waveguide ports excitation.

Entrance of the coaxial probes and the dimensions of U-shape slots are critical for the return loss performance of the SIW hybrid ring in the next section. A lot of simulations have been made to optimize the transitional performance using CST, which the optimized dimensions are demonstrated in Fig. 1. By applying these coupling slots over the top plate of SIW transition, the TEM waves from coaxial cables convert to TE<sub>10</sub>-like modes and enter into SIW structure. Thus, the performance of this proposed structure is the same as the structure when excited only with waveguide ports. This agreement is illustrated in Fig. 2. As shown in the figure, the  $S_{11}$  and  $S_{21}$  of the structure in fundamental mode when excited with coaxial cable and U-shape slot-coupled are similar to waveguide port excitation. We use this similarity in our analysis in Section IV.

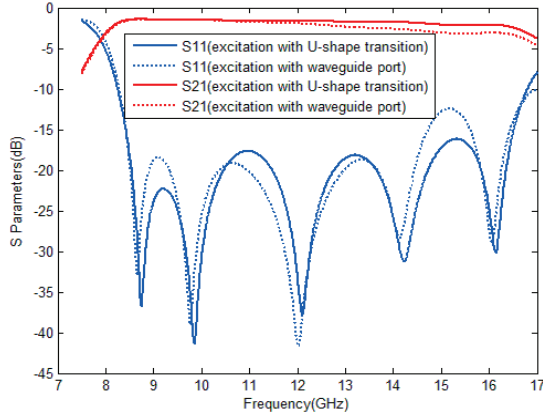


Fig. 2. S-parameters of SIW structure with waveguide port excitation and U-shape slot-coupled transition.

### III. DESIGN AND OPTIMIZATION PROCEDURE OF SIW HYBRID RING (RAT-RACE) COUPLER

The optimized SIW hybrid ring (rat-race) structure has been shown in Fig. 3. The dimension of the proposed coupler has been obtained based on the following procedure:

1. In the previous section, we have designed a new SIW transition which is applied for excitation of our coupler. As shown in Fig. 3, the SIW coupler arms consist of four U-shape slots and coaxial connectors.
2. According to [23] for manufacturing considerations, the distances between the four arms should be increased one wavelength in comparison to conventional distances between the coupler arms. The spatial angles between the four ports have been shown in Fig. 3.
3. We have chosen the logical and possible ranges for inner radius ( $r1$ ),  $3 \leq r1 \leq 9$  and outer radius ( $r3$ ),  $10 \leq r3 \leq 20$  of the coupler. In addition, four matching posts have been used for improving the impedance matching of the coupler [23]. The initial radius ( $r2$ ) of the matching posts is in  $3.5 \leq r2 \leq 9.5$  range. By choosing three radiuses from above ranges, our initial coupler has been prepared for analysis. The SIW rat-race coupler analysis has been presented in detail in the next section.
4. After calculating the coupler S-parameters form analysis, we have optimized the coupler with IWO optimization algorithm [24]. The

parameters under optimization are  $r1$ ,  $r2$ ,  $r3$  and the matching posts diameters. In our optimization, the operating frequency band was over 8.5-16 GHz, but because of considering all goal functions, i.e., return loss, isolation, insertion loss and phase differences of the coupler; simultaneously the maximized bandwidth has been met 30% relative bandwidth, which is over 11-15 GHz for our optimized dimensions in Fig. 3. To the best of our knowledge, this relative bandwidth has not been obtained for the SIW rat-race coupler by literatures up to now, and the proposed SIW rat-race coupler is a good candidate for the wideband applications because the relative bandwidth of the coupler can be shifted in the interested band by changing and optimizing the dimensions.

Also, because of using the probe feeding instead of the microstrip line transition, our coupler is low loss and profile. The experimental measurements confirm our claim in Section V.

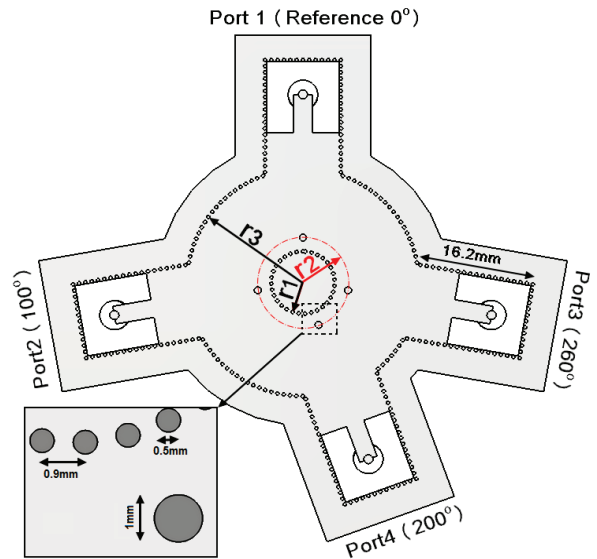


Fig. 3. The SIW hybrid ring coupler structure ( $r1=4.5$  mm,  $r2=6.5$  mm and  $r3=15.5$  mm).

### IV. SIW HYBRID RING (RAT-RACE) COUPLER ANALYSIS

In this section, we analyze the SIW hybrid ring (rat-race) coupler with mode matching algorithm for these reasons:

- a. Our analysis minimizes memory computation and time consumption rather than the other

- full wave package like CST and HFSS.
- b. As mentioned in the previous section, after calculating the S-parameters of the coupler from our analysis, we can optimize the dimensions of the coupler to achieve the higher bandwidth with optimization algorithms through Matlab code, whereas the optimization of the SIW coupler takes a very long time in CST or HFSS. Furthermore, after many optimizations in CST or HFSS, the goal functions for this SIW coupler is not capable of reaching to our desired bandwidth.
- c. It is worthwhile mentioning that our code can generally be handled for the SIW passive structures which require bandwidth enhancing and the analyzed and optimized algorithm have been applied for the proposed SIW coupler as a good example in our effort.

According to Section II, because the coaxial cable TEM waves are converted to TE modes through the U-shape slots, to analyze the fields in the SIW Hybrid ring (rat-race) structure, we substitute four U-shape slots and coaxial cables with rectangular waveguide port excitations (magnetic source in this paper).

Now, we can examine the incident and scattered magnetic fields from each metallic post included vias of four rectangular arms, four matching posts with radius ( $r_2$ ), vias of inner radius ( $r_1$ ) and vias of the outer radius ( $r_3$ ) of the SIW coupler. In general, an arbitrary total magnetic field  $H(r)$  can be expressed as:

$$H_{total}(r) = H_1 + H_2, \quad (1)$$

where  $H_1$  is incident wave from a magnetic source ( $M'_s$ ) and  $H_2$  is scattering magnetic wave from each via. Calculating  $H_1$ , we need this equation:

$$H_1 = -j\omega\epsilon \iiint_{V'} G_{m2} M'_s dV', \quad (2)$$

where  $G_{m2}$  is a magnetic Green's function of the second kind, which for parallel plate waveguide through using residue theorem in cylindrical coordination and [25,26], explicit form is given by:

$$\begin{aligned} G_{m2}(r, r') &= \frac{\hat{\rho}\hat{\rho}'}{k^2} \delta(r-r') \\ &- \frac{1}{j4\pi} \sum_{m=0}^{N_s} \sum_{n=-N_s}^{N_s} (2-\delta_{m0}) \frac{1}{k_m^2 h} \times \\ &[P_n(k_m, k_z, \rho, z) P'_n(k_m, k_z, \rho', z) + \\ &Q_n(k_m, k_z, \rho, z) Q'_n(k_m, k_z, \rho', z)] \quad \rho > \rho', \end{aligned} \quad (3)$$

and

$$\delta_{m0} = \begin{cases} 0 & \text{if } m \neq 0 \\ 1 & \text{if } m = 0 \end{cases}$$

In (3), we define two vector wave functions  $P_n(k_m, k_z, \rho, z)$  and  $Q_n(k_m, k_z, \rho, z)$  as the equivalence of magnetic fields. Calculating these functions, lets assume this harmonic scalar potential  $\mathcal{G}_n(r)$ :

$$\mathcal{G}_n(r) = \begin{cases} H_n^{(2)}(k_m \rho) e^{j(k_z z - n\phi)} & \rho > \rho' \\ J_n(k_m \rho) e^{-j(k_z z - n\phi)} & \rho \leq \rho' \end{cases}, \quad (4)$$

where  $H_n^{(2)}$  and  $J_n$  indicate  $n$ -order Hankel's function of the second kind and  $n$ -order Bessel's function respectively. Also,  $k_m = \sqrt{k^2 - k_z^2}$ ,  $k_z = m\pi/h$ ,  $k = \omega\sqrt{\mu_0\epsilon_0\epsilon_r}$  and  $h$  is the height of substrate. In this manner,  $m$  and  $n$  are the cylindrical modes in vertical ( $z$  direction) and azimuthally ( $\phi$  direction) respectively.

The relation between  $P_n(k_m, k_z, \rho, z)$  and  $Q_n(k_m, k_z, \rho, z)$  is as follows:

$$P_n(k_m, k_z, \rho, z) = \nabla \times (\mathcal{G}_n(r) \hat{\rho}), \quad (5.a)$$

$$Q_n(k_m, k_z, \rho, z) = \frac{1}{k} \nabla \times P_n(k_m, k_z, \rho, z), \quad (5.b)$$

where  $\hat{\rho}$  is unit normal vector on the lateral surface of each cylindrical metallic post of the hybrid ring coupler. Similarly,  $P'_n(k_m, k_z, \rho', z)$  and  $Q'_n(k_m, k_z, \rho', z)$  can be acquired from (5.a) and (5.b) by interchanging  $\rho \leq \rho'$  within (4).

We can write scattering waves for TM and TE modes as Cylindrical Vector Wave (CVW) expansions:

$$\begin{aligned} H_2(r) &= \sum_{l=1}^{P_{via}} \sum_{m=1}^{N_z} \sum_{n=0}^{N_\phi} [C_{l,m,n}^{TM} P_n(k_m, k_z, \rho, z) \\ &+ D_{l,m,n}^{TE} Q_n(k_m, k_z, \rho, z)], \end{aligned} \quad (6)$$

where index  $l$  denotes to the number of the SIW coupler vias. To determine unknown coefficients ( $C_{l,m,n}^{TM}, D_{l,m,n}^{TE}$ ), the boundary conditions should be imposed for the surface of each via; for metallic (PEC) vias:

$$\begin{aligned} n \times (E_1 + E_2) &= 0 \\ &\text{in surface of each PEC with radius } a_i, \end{aligned} \quad (7)$$

where  $(E_1 + E_2) = (1/j\omega\epsilon)\nabla \times (H_1 + H_2)$  and  $a_i$  is each metallic via radius of the coupler as the radiuses of the four matching posts are twice of the other vias in Fig. 3.

By operating (7), the unknown coefficient vector  $F_{l,m,n}^{TM/TE} = [C_{l,m,n}^{TM}, D_{l,m,n}^{TE}]$  can be expressed as:

$$\begin{bmatrix} F_{1,1,0}^{TM/TE} \\ \vdots \\ F_{l,m,n}^{TM/TE} \end{bmatrix} = [U]^{-1}[S], \quad (8)$$

where  $U$  and  $S$  are interaction matrix between the vias and excitation vector respectively.

After determining the coefficients from (8), we use the admittance matrix of rectangular waveguide [27] which is replaced with coaxial cable and U-shape slot coupling:

$$Y_{i,j} = j\omega\epsilon Z_i Z_j \iint G_{m2}(r_i, r_j) h^i h^j dS_i dS_j + Z_i \int H_2^j(r) h^i dS_i, \quad (9)$$

where  $h^i$  and  $h^j$  are magnetic field modal vector and  $Z_i$ ,  $Z_j$  are wave impedance for each waveguide port. If we regard cross section of the SIW coupler waveguide port in the x-direction with the equivalent width of waveguide port  $a_{eqv}$  and y-direction with the substrate height  $h$ , for TE mode,  $h^i$  or  $h^j$  in (9) is obtained as:

$$h^{TE} = \frac{-2}{(m^2 \frac{h}{a_{eqv}} + n^2 \frac{a_{eqv}}{h})^{\frac{1}{2}}} \hat{n}^p \times \left[ \frac{m}{a_{eqv}} \cos(\frac{m\pi}{a_{eqv}} x) \sin(\frac{n\pi}{h} y) \hat{x} + \frac{n}{h} \sin(\frac{m\pi}{a_{eqv}} x) \cos(\frac{n\pi}{h} y) \hat{y} \right]. \quad (10)$$

Similarly for TM mode,

$$h^{TM} = \frac{(\epsilon_m \epsilon_n)^{1/2}}{(m^2 \frac{h}{a_{eqv}} + n^2 \frac{a_{eqv}}{h})^{\frac{1}{2}}} \hat{n}^p \times \left[ \frac{n}{h} \cos(\frac{m\pi}{a_{eqv}} x) \sin(\frac{n\pi}{h} y) \hat{x} - \frac{m}{a_{eqv}} \sin(\frac{m\pi}{a_{eqv}} x) \cos(\frac{n\pi}{h} y) \hat{y} \right]. \quad (11)$$

In (10) and (11):

$$m, n = 0, 1, 2, 3, \dots, m = n = 0 \text{ is excluded,}$$

and

$$\epsilon_k = \begin{cases} 1 & \text{if } k = 0 \\ 2 & \text{if } k \neq 0 \end{cases}$$

where  $\hat{n}^p$  denotes the unit normal vector to the waveguide port.

From the knowledge of the admittance matrix, the scattering matrix of the SIW coupler can

simply be computed [28].

## V. RESULTS AND DISCUSSION

The proposed algorithm in Section IV has been implemented in Matlab code. The TE10 mode propagation is considered for all the waveguide ports of the analyzed SIW coupler.

Attaining to 0.01 error of the coupler parameters,  $N_\phi=7$  and  $N_z=2$  cylindrical modes in (3) and (6) have been selected, and the obtained results are validated with the simulation and experimental conclusions.

In our attempt, the substrate material and the thickness are Rogers R04003 with  $\epsilon_r=3.55$  and  $h=0.813$  mm in the order mentioned. Figure 4 depicts a manufactured SIW rat-race coupler with the dimensions which have been acquired in Section III.

The coupler S-parameters from the analysis, CST time domain solver and measurement are shown in Figs. 5 and 6. From Fig. 5 (a), the return losses ( $S_{11}$ ) and isolations ( $S_{41}$ ) are less than -18 dB and -20 dB over 11-15 GHz (30% relative bandwidth) respectively. In addition, the insertion losses between the output ports, ports 2 and 3, are divided equally from -3-1.7 dB to -3 + 1 dB in Fig. 5 (b). As shown in Fig. 6, throughout 11-15 GHz, the phase differences between ports 2 and 3 for in-phase are in the range of  $0^\circ-4.7^\circ$  to  $0^\circ+2.1^\circ$ , when port 4 is excited and for out-of-phase are from  $180^\circ-4^\circ$  to  $180^\circ+2.5^\circ$ , when port 1 is excited. Obviously, very good agreement has been obtained from our method, simulation and measurement which this matter confirms accuracy of the proposed analysis.

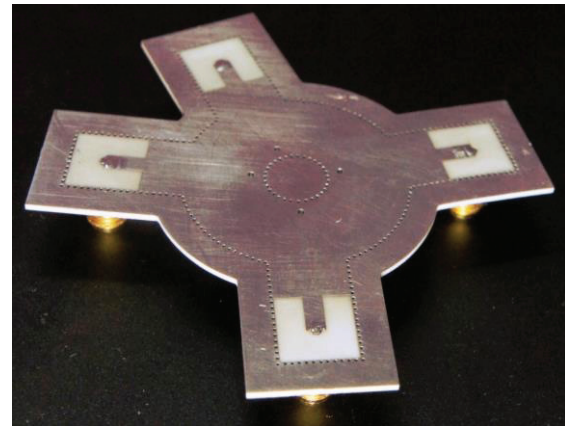


Fig. 4. The photograph of the manufactured SIW rat-race (hybrid ring) coupler.

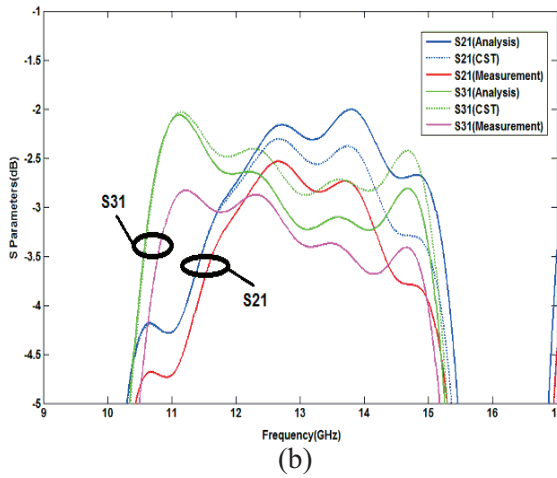
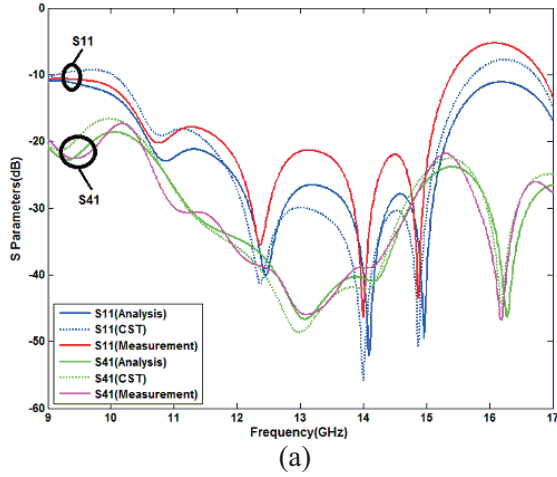


Fig. 5. Comparison of the SIW hybrid ring coupler S-parameters: (a) return loss ( $S_{11}$ ) and isolation ( $S_{41}$ ), and (b) insertion losses ( $S_{21}$  and  $S_{31}$ ).

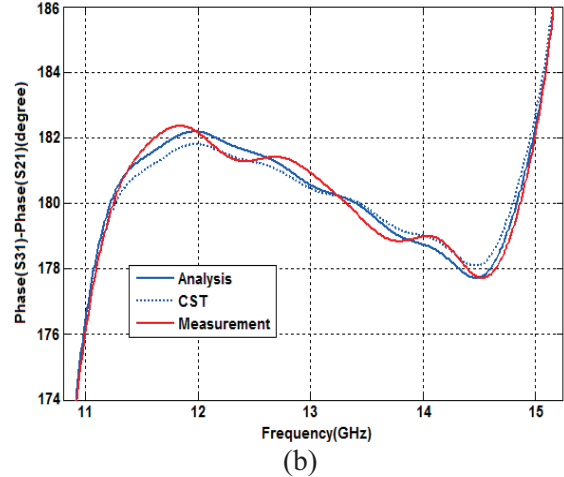
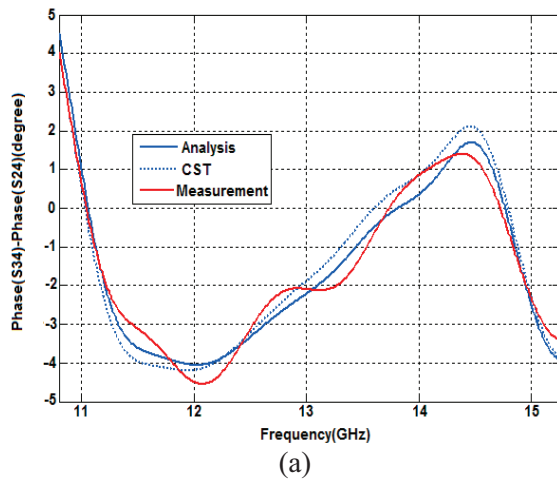


Fig. 6. The phase difference responses: (a) in-phase response, and (b) out-of-phase response.

To prove the efficiency of our analysis, the coupler has been compared with HFSS and CST frequency domain solver as well as CST time domain solver. In the case of analysis, HFSS and CST frequency domain solver, the allowed error for the S-parameters convergence of the coupler is 1% and we have used 50 frequency points for the output results. After calculating the all frequency points, the run time ratio of the analysis is related to HFSS is 1/21 and CST frequency domain solver is 1/20, while to CST time domain solver is 1/12.5 ratio. So, our method has the best efficiency and the CST time domain solver efficiency is much closer to the analysis rather than HFSS or CST frequency domain. Table 1 has reported the simulation time of the proposed coupler from the analysis, CST and HFSS.

Table 1: Simulation time on a Core i5 with 4-GB RAM (azimuthally mode numbers=7, vertically mode numbers=2)

Structure Type	Vias Number	CST CPU Time	HFSS	Analysis
		Time Domain	Frequency Domain	50 Frequency Points
SIW Hybrid ring (rat-race) coupler	324	1500s	2520s	120s

## VI. CONCLUSION

This paper presents a novel SIW transition as an application for the SIW hybrid ring (rat-race) coupler under analysis. By using U-shape slot-coupled transitions, the relative bandwidth of the rat-race coupler has been increased up to 30% with low loss, low profile and high isolation in the operated frequency. This hybrid ring coupler has been analyzed with an efficient and accurate method of mode matching to calculate the scattering matrix. The output parameters of the analyzed and optimized coupler have been justified with full wave simulation and experimental results. Without losing the generality of the analysis, our method is a good candidate for the relative bandwidth improving (up to 30 percent) of the other passive SIW structures.

## REFERENCES

- [1] K. Wu, D. Deslandes, and Y. Cassivi, "The substrate integrated circuits-a new concept for high-frequency electronics and optoelectronics," *In Proc. 6<sup>th</sup> International Conference on Telecommunications in Modern Satellite, Cable and Broadcasting Service TELSIKS 2003*, vol. 1, pp. P-III-P-X, 2003.
- [2] Z. Q. Xu, P. Wang, J. X. Liao, and Y. Shi, "Substrate integrated waveguide filter with mixed coupled modified trisections," *IET Electronic Letter*, vol. 49, pp. 482-483, March 2013.
- [3] H. Min-Hua and L. Cheng-Siou, "Novel balanced bandpass filters using substrate integrated half-mode waveguide," *IEEE Microwave and Wireless Component Letters*, vol. 23, pp. 78-80, February 2013.
- [4] Z. Li, M. S. Mahani, and R. Abhari, "Experiment of substrate integrated waveguide interconnect measurement for high speed data transmission application," *Microw. Opt. Technol. Lett.*, vol. 54, no. 2, pp. 401-405, February 2012.
- [5] F. Giuppi, A. Georgiadis, A. Collado, and M. Bozzi, "Active substrate integrated waveguide (SIW) antenna with phase-shifterless beam-scanning capabilities," *IEEE MTT-S Int. Microwave Symp. Dig.*, pp. 1-3, June 2012.
- [6] E. Ofli, R. Vahldieck, and S. Amari, "Novel E-plane filters and diplexers with elliptic response for millimeter-wave applications," *IEEE Trans. Microw. Theory Tech.*, vol. 53, no. 3, pp. 843-851, March 2005.
- [7] W. M. Abdel-Wahab and S. Safavi-Naeini, "Low loss double-layer substrate integrated waveguide-hybrid branch line coupler for mm-wave antenna arrays," *IEEE Antennas and Propagation International Society Symposium (APSURSI)*, pp. 2074-2076, 2011.
- [8] K. Song, F. Zhang, F. Chen, and Y. Fan, "Wideband millimetre-wave four-way spatial power combiner based on multilayer SIW," *Journal of Electromagnetic Waves and Applications*, vol. 27, nos. 13, 1715-1719, 2013.
- [9] Y. Liu, X. H. Tang, and T. Wu, "SIW-based low phase-noise millimeter-wave planar dual-port voltage-controlled oscillator," *Journal of Electromagnetic Waves and Applications*, vol. 27, nos. 8-9, 1059-1069, 2012.
- [10] T. Kai, J. Hirokawa, and M. Ando, "Transformer between a thin postwall waveguide to a standard metal waveguide," *In IEEE Antennas Propagation Society Symp. Dig.*, pp. 436-439, June 2002.
- [11] D. Deslandes and K. Wu, "Integrated microstrip and rectangular waveguide in planar form," *IEEE Microw. Wireless Compon. Lett.*, vol. 11, no. 2, pp. 68-70, February 2001.
- [12] N. Jain and N. Kinayman, "A novel microstrip mode to waveguide mode transformer and its applications," *In IEEE MTT-S Int. Microwave Symp. Dig.*, pp. 623-626, May 2001.
- [13] Y. Huang, K. L. Wu, and M. Ehlert, "An integrated LTCC laminated waveguide-to-microstrip line T-junction," *IEEE Microw. Wireless Compon. Lett.*, vol. 13, no. 8, pp. 338-339, August 2003.
- [14] S. Lin, A. E. Fathy, and A. Elsherbini, "Development of a novel UWB vivaldi antenna array using SIW technology," *Progress In Electromagnetics Research, PIER 90*, 369-384, 2009.
- [15] R. Kazemi, A. E. Fathy, S. Yang, and R. A. Sadeghzadeh, "Development of an ultra-wide band GCPW to SIW transition," *IEEE Radio and Wireless Symposium (RWS)*, pp. 171-174, January 2012.
- [16] E. D. Caballero, H. Esteban, A. Belenguer, and V. Boria, "Efficient analysis of substrate integrated waveguide devices using hybrid mode matching between cylindrical and guided modes," *IEEE Trans. Microw. Theory Tech.*, vol. 60, no. 2, pp. 232-243, February 2012.
- [17] A. Belenguer, H. Esteban, E. Diaz, C. Bachiller, J. Cascon, and V. E. Boria, "Hybrid technique plus fast frequency sweep for the efficient and accurate analysis of substrate integrated waveguide devices," *IEEE Trans. Microw. Theory Tech.*, vol. 59, no. 3, pp. 552-560, March 2011.
- [18] E. Arneri and G. Amendola, "Analysis of substrate integrated waveguide structures based on the parallel-plate waveguide green's function," *IEEE Trans. Microw. Theory Tech.*, vol. 56, no. 7, pp. 1615-1623, July 2008.
- [19] B. Wu and L. Tsang, "Full-wave modeling of

multiple vias using differential signaling and shared antipad in multilayered high speed vertical interconnects,” *Progress In Electromagnetics Research, PIER 97*, 129-139, 2009.

- [20] M. Casaletti, R. Sauleau, and M. Ettore, “Efficient analysis of metallic and dielectric posts in parallel-plate waveguide structures,” *IEEE Trans. Microw. Theory Tech.*, vol. 60, no. 10, pp. 2979-2989, October 2012.
- [21] E. Arneri and G. Amendola, “Method of moments analysis of slotted substrate integrated waveguide arrays,” *IEEE Trans. Antennas Propag.*, vol. 59, no. 4, pp. 1148-1154, April 2011.
- [22] H. Zairi, H. Baudrand, A. Gharsalla, and A. H. Gharb, “An efficient iterative method for analysis of a substrate integrated waveguide structures,” *Microw. Opt. Technol. Lett.*, vol. 52, no. 1, pp. 45-48, January 2010.
- [23] W. Che, K. Deng, E. K. N. Yung, and K. Wu, “H-plane 3-dB hybrid ring of high isolation in substrate integrated rectangular waveguide (SIRW),” *Microw. Opt. Technol. Lett.*, vol. 48, no. 3, pp. 502-505, March 2006.
- [24] A. R. Mehrabian and C. Lucas, “A novel numerical optimization algorithm inspired from weed colonization,” *Ecological Informatics*, vol. 1, 355-366, 2006.
- [25] C. T. Tai, “Generalized vector and dyadic analysis: applied mathematics in field theory,” series on Electromagnetic Waves, Piscataway, *IEEE Press*, 1991.
- [26] C. T. Tai, “Dyadic green’s function in electromagnetic theory,” series on Electromagnetic Waves, Piscataway, *IEEE Press*, 1993.
- [27] R. E. Collin, “Field theory of guided waves,” series on Electromagnetic Waves, Piscataway, *IEEE Press*, 1993.
- [28] D. M. Pozar, “Microwave engineering,” 3<sup>rd</sup> edition, *John Wiley & Sons Inc.*, 2005.



**Ramin Dehdasht-Heydari** was born in Esfahan-Iran, in 1983. He received the B.Sc. and M.Sc. degrees in Electrical Eng. in 2005 and 2008 from the Shahid Sattari and Shahed Universities, Tehran-Iran, respectively. He currently is pursuing his Ph.D.

thesis with the Science & Research Branch, Islamic Azad University, Tehran-Iran. His principal fields of interest in research are UWB antennas, microwave and millimeter wave circuits, and numerical electromagnetism methods.



**Keyvan Forooghi** received the M.Sc. degree in Electrical Engineering, the Licentiate of Technology degree and the Ph.D. degree in Electrical Engineering in 1991 from Chalmers University of Technology, Gothenburg, Sweden. He worked as a Researcher at

Chalmers University of Technology from 1991 to 1992. In 1992, he joined the Department of Computer and Electrical Engineering, Tarbiat Modares University. Presently he is a Full Professor with the

Communication Group. His research interests include electromagnetic theory and computational electromagnetic and antenna theory.



**Mohammad Naser-Moghadasi** was born in Saveh, Iran, in 1959. He received the B.Sc. degree in Communication Eng. in 1985 from the Leeds Metropolitan University, UK. From 1987 to 1989, he was awarded a full scholarship by the Leeds Educational Authority to pursue an M.Phil. studying in CAD of Microwave Circuits.

He received his Ph.D. in 1993, from the University of Bradford, UK. He was offered then a two years Post Doc. to pursue research on Microwave cooking of materials at the University of Nottingham, UK. In 1995, Naser-Moghadasi joined Islamic Azad University, Science & Research Branch, Iran, where he currently is an Associate Professor and Head of Postgraduate Studies.

His main areas of interest in research are Microstrip antenna, Microwave passive and active circuits, RF MEMS. He has so far published over 140 papers in different journals and conferences.